Origin of low Gilbert damping in half metals

Chunsheng Liu,[1] Claudia K. A. Mewes,[1,a)] Mairbek Chshiev,[2] Tim Mewes,[1] and William H. Butler[1]
[1]*Department of Physics and Astronomy and Center for Materials for Information Technology, University of Alabama, Box 870209, Tuscaloosa, Alabama 35487, USA*
[2]*Spintec, CEA/CNRS, 38054 Grenoble, France*

(Received 6 April 2009; accepted 1 June 2009; published online 14 July 2009)

Using a combination of first-principles calculations and an extended Hückel tight binding model this letter reports on the origin of the low Gilbert damping in half metals. This approach enables the prediction of the lower limit for the magnetization relaxation in a wide variety of material systems relevant for future spintronic applications. For the two model systems Co_2MnGe and Co_2MnSi minimal damping parameters of 1.9×10^{-4} and 0.6×10^{-4} are predicted. © *2009 American Institute of Physics*. [DOI: 10.1063/1.3157267]

The understanding of magnetic damping in metals has been a long standing problem in solid state physics. Until recently, damping in magnetic systems was usually treated as a phenomenological parameter that entered the Landau–Lifshitz–Gilbert (LLG) equation including a damping term[1]

$$\frac{d\boldsymbol{M}}{dt} = -\gamma\boldsymbol{M}\times\left[\boldsymbol{H}_{\mathrm{eff}} - \frac{\lambda}{(\gamma M)^2}\frac{d\boldsymbol{M}}{dt}\right], \tag{1}$$

where $\boldsymbol{M}$ is the macroscopic magnetization, $\boldsymbol{H}_{\mathrm{eff}}$ is the effective field, and γ is the gyromagnetic ratio. The first term describes the precession of $\boldsymbol{M}$ about the effective field, whereas the second term accounts for the damping phenomenologically. λ is the Landau–Lifshitz (LL) damping rate, which is connected to the dimensionless Gilbert damping constant[2,3] $\alpha=\lambda/\gamma M$.

Recently Gilmore *et al.*[4,5] determined the dominant damping mechanism in the transition metals Fe, Co, and Ni using first-principles calculations. Similar calculations were performed by Kamberský.[6] Both sets of calculations used the torque-correlation model of Kamberský and co-workers.[7–9] Calculations of intrinsic magnetic damping using first principles alone, however, require a huge amount of computational power even for simple structures such as transition metals. In order to make these calculations more tractable, transparent, and applicable to materials of current interest, we have combined first-principles calculations with an extended Hückel tight binding (ETH-TB) model[10–12] and applied this approach to the case of Heusler alloys highlighting their potential as low damping materials for spintronics.

Kamberský's torque correlation model describes damping in terms of spin orbit torque correlations in the one-electron model, predicting the experimentally observed temperature dependence of the damping rate in transition metals which shows a minimum as a function of temperature, which is caused by conductivity-like and resistivity-like contributions.[13,14]

Within the framework of Kamberský's torque correlation model, the damping rate is given by

$$\lambda = \frac{\mu_0 g^2 \mu_B^2}{\hbar}\frac{\pi^2/2}{\Omega_{\mathrm{at}}}\left\langle \sum_{m,n} |\Gamma^-_{m\boldsymbol{k},n\boldsymbol{k}}|^2 W_{m\boldsymbol{k},n\boldsymbol{k}} \right\rangle_{\boldsymbol{k}}, \tag{2}$$

where g is the Landé g factor, μ_0 is the permeability of free space, Ω_{at} is the atomic volume, μ_B is the Bohr magneton, n and m are band indices, and $\boldsymbol{k}$ is the electron wave vector. $\langle\,\rangle_{\boldsymbol{k}}$ denotes the average over the first Brillouin zone.

The transitions between states in bands n and m induced by the torque between spin and orbital moments during precession are described by the transition matrix elements $\Gamma^-_{m\boldsymbol{k},n\boldsymbol{k}}=\langle m,\boldsymbol{k}|[\sigma^-,\mathcal{H}_{\mathrm{SO}}]|n,\boldsymbol{k}\rangle$ and are weighted by the spectral overlap function $W_{m\boldsymbol{k},n\boldsymbol{k}}(\boldsymbol{k})=1/\pi\int dE\,\eta(E)\langle D(E_{m\boldsymbol{k}})\rangle \times\langle D(E_{n\boldsymbol{k}})\rangle$. Here $\eta(E)$ is the negative derivative of the Fermi function and restricts the integral over spectral overlap functions to energies within a few times k_BT around the Fermi level. $\langle D(E_{m\boldsymbol{k}})\rangle=(1/\pi)\delta/[(E-E_{m\boldsymbol{k}})^2+\delta^2]$ is the averaged spectral density of states (DOS). The width $\delta=\hbar/(2\tau)$ of those functions is defined by the orbital or "Bloch state" lifetime τ and accounts phenomenologically for the role of electron-lattice scattering processes.

The scattering events within a single band ($n=m$) result in a spectral overlap proportional to the scattering time τ and are called intraband transitions. They lead to the conductivity-like damping term. For the transition between two different bands ($m\neq n$), the interband transitions, the spectral overlap shows a roughly inverse proportionality to the scattering time and results in the resistivity-like term.[4]

One subclass of half-metallic materials, which is of particular interest, is full Heusler alloys X_2YZ of structure type $L2_1$. The elements X and Y are typically transition metals and the Z element is a nontransition metal. Due to their high Curie temperature, the alloys Co_2MnSi and Co_2MnGe are of special interest within this subclass of half-metallic structures. To investigate the properties of these materials, first-principles calculations using density functional theory within the generalized gradient approximation as implemented in the Vienna *ab initio* simulation package[15] were performed. Calculations which do not include spin orbit coupling show minority gaps at the Fermi energy of 0.59 eV for Co_2MnSi and 0.35 eV for Co_2MnGe. We also calculated the energy bands including spin orbit coupling; these results were used to build the ETH-TB model in which a minimal *spd* basis set per element is employed while each atomic orbital is described by a double-ζ Slater-type wave function. The energy

a)Electronic mail: cmewes@mint.ua.edu.

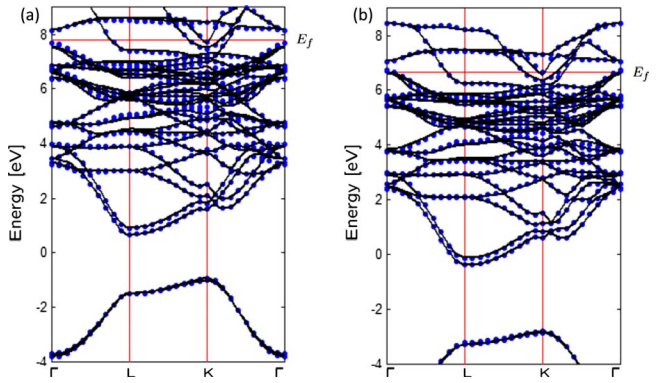

FIG. 1. (Color online) Band structure along symmetry lines for (a) Co_2MnSi and (b) Co_2MnGe. The lines show the result from the first-principles calculations. The overlayed dots show the band structure obtained within the ETH-TB model. In both cases spin orbit interaction has been taken into account.

bands within the ETH-TB theory may be obtained by the solution of the secular determinant $|\mathcal{H}_{ij}(\boldsymbol{k})-\mathcal{S}_{ij}(\boldsymbol{k})E|=0$, where $\mathcal{H}_{ij}$ are the components of the Hamiltonian and $\mathcal{S}_{ij}=\langle\chi_i|\chi_j\rangle$ is the overlap integral linking the atomic basis orbitals χ_i and χ_j. The "on-site" integrals $\mathcal{H}_{ii}=\langle\chi_i|\hat{\mathcal{H}}|\chi_i\rangle$ are free fitting parameters, whereas the interaction integrals are expressed in the Mulliken approximation[16,17] $\mathcal{H}_{ij}=\langle\chi_i|\hat{\mathcal{H}}|\chi_j\rangle=\frac{1}{2}K\mathcal{S}_{ij}(\mathcal{H}_{ii}+\mathcal{H}_{jj})$, where K is a constant.

In addition to the one on-site integral per orbital, there are three parameters per orbital that govern its shape and extent. The ETH-TB parameters are obtained through a fit to the first-principles band structure throughout the first Brillouin zone. The spin orbit interaction is included through an addition to the Hamiltonian $H_{SO}=\xi\boldsymbol{L}\cdot\boldsymbol{S}$, where ξ is the spin orbit coupling parameter, which is an additional fitting parameter. A comparison of the band structures obtained with first-principles approaches and the EHT-TB model along certain symmetry directions is shown in Figs. 1(a) and 1(b). The good fit is particularly significant since these k-points were not used during the fitting procedure.

The spin orbit coupling parameters for Co_2MnSi and Co_2MnGe are 0.043 and 0.052 eV, respectively. The resulting ETH-TB model was used to evaluate Eq. (2) with sampling of $(100)^3$ k points in the first Brillouin zone to guarantee the convergence of the result. Within the ETH-TB model it is possible to evaluate the matrix elements $\Gamma^{-}_{mk,nk}$ in the basis of atomlike double-ζ Slater-type orbitals centered at $\boldsymbol{R}$. We used the same procedure to calculate the damping for the transition metal Fe obtaining a result in agreement with the first-principles results of Gilmore *et al.*[4] and Kamberský.[6]

To facilitate the comparison with experiments the calculated damping constants for the $L2_1$ half metals Co_2MnSi and Co_2MnGe are shown as a function of the electrical resistivity in Figs. 2(a) and 2(b). The resistivity was calculated within a semiclassical approximation to replace the averaged Bloch state lifetime τ in the damping calculation. Here the electric conductivity tensor is given by $\hat{\sigma}=\tau(e^2/\Omega_{at})\Sigma_{\boldsymbol{k}}\eta(E)\boldsymbol{v}_{\boldsymbol{k}}\circ\boldsymbol{v}_{\boldsymbol{k}}$ with the group velocity $\boldsymbol{v}_{\boldsymbol{k}}=\partial E(\boldsymbol{k})/\hbar\,\partial\boldsymbol{k}$. The derivatives of the energy bands can be easily calculated within the TB model.[19]

The minimum intrinsic relaxation rate λ corresponds to an extremely low LLG damping constant $\alpha=\lambda/(\gamma M_s)$ of 0.6×10^{-4} and 1.9×10^{-4} for Co_2MnSi and Co_2MnGe, respectively. These are more than an order of magnitude smaller than the minimum damping rate for the transition metals. These extremely low damping rates can be understood using the analytical expression for the absolute square of the transition matrix element $|\Gamma^{-}_{mk,nk}|^2$. It can be expressed as a product of two sums consisting of double products of expansion coefficients of the double-ζ Slater-type orbital basis set. Considering only the spin index the transition matrix element can be expressed symbolically as the absolute square of the sum of three spin dependent contributions from which two are determined by spin-preserving transitions and one is determined by a spin-flip transition

$$|\Gamma^{-}_{mk,nk}|^2=\langle m,\boldsymbol{k}|[\sigma^{-},\mathcal{H}_{SO}]|n,\boldsymbol{k}\rangle\equiv|S^{\uparrow\uparrow}_{mn}(\boldsymbol{k})+S^{\downarrow\uparrow}_{mn}(\boldsymbol{k})+S^{\downarrow\downarrow}_{mn}(\boldsymbol{k})|^2. \tag{3}$$

In the ETH-TB model those three coefficients can be explicitly evaluated. Due to the nature of the torque operator $[\sigma^{-},\mathcal{H}_{SO}]=\hat{L}_z\hat{S}_{-}-\hat{L}_{-}\hat{S}_z$, where $\hat{L}_z$, $\hat{L}_{-}=\hat{L}_x-i\hat{L}_y$, $\hat{S}_z$, and $\hat{S}_{-}=\hat{S}_x-i\hat{S}_y$ are the conventional angular momentum and spin operators, only certain states can contribute. The operator $\hat{L}_{-}\hat{S}_z$ leaves the spin state unchanged and therefore determines the two spin-conserving contributions, whereas the operator $\hat{L}_z\hat{S}_{-}$ accounts for all spin-flip contributions. Regarding also the restrictions imposed by the momentum operator this leads to six different contributions to the spin-flip transitions and 16 contributions for the spin-conserving transition for each spin channel. Assuming that each of those contributions accounts with the same order of magnitude to

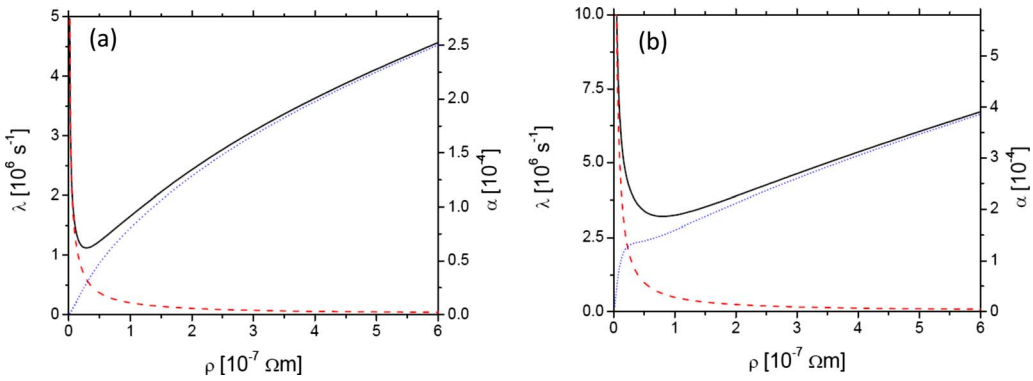

FIG. 2. (Color online) LL damping parameter for (a) Co_2MnSi and (b) Co_2MnGe as a function of the electric resistivity. The total damping parameter corresponds to the solid line. The intraband and the interband contributions correspond to the dashed and dotted curves. Typical experimental values for the resistivity of Co_2MnSi are 7 $\mu\Omega$ cm at 5 K and 20 $\mu\Omega$ cm at room temperature (Ref. 18).

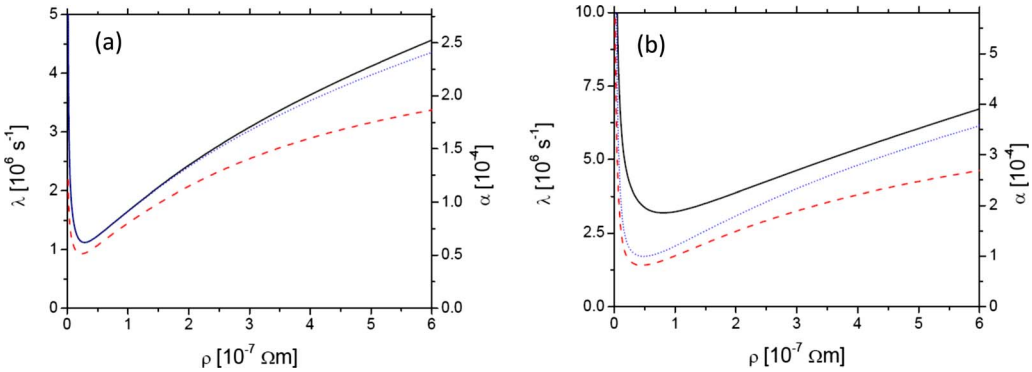

FIG. 3. (Color online) LL damping parameter as a function of the electric resistivity for (a) Co_2MnSi and (b) Co_2MnGe. The solid curve shows the total damping parameter as a reference. The dashed line shows the damping constant neglecting the summands $S_{mn}^{\downarrow\downarrow}(\boldsymbol{k})$ in the transition matrix element Γ_{mknk} and the dotted line shows the damping constant where only contributions from $S_{mn}^{\uparrow\uparrow}(\boldsymbol{k})$ are taken into account.

the damping and assuming that all components which involve contributions from the down spin channel can be set to zero in a half metal this leads to an estimated reduction in the damping parameter by a factor of ~0.18. This simple picture only holds in the limit of no spin orbit coupling. Spin orbit coupling mixes the majority (↑) and the minority (↓) components of the Bloch states and therefore the contributions involving minority spin states cannot be neglected completely. Their contribution depends strongly on the spin polarization at the Fermi level as well as on the spin orbit coupling strength. The spin orbit coupling of the two spin channels is related to the unperturbed potential around each atom through the angular momentum operator and the Pauli spin matrix and can be expressed in spinor basis

$$\mathcal{H}_{\mathrm{SO}} = \begin{pmatrix} V_{\mathrm{SO}}^{\uparrow\uparrow} & V_{\mathrm{SO}}^{\uparrow\downarrow} \\ V_{\mathrm{SO}}^{\downarrow\uparrow} & V_{\mathrm{SO}}^{\downarrow\downarrow} \end{pmatrix}.$$

Mavropoulos *et al.*[20,21] showed using perturbation theory that within the gap region of the half metal the minority DOS has in first order a quadratic dependence on the spin orbit coupling strength $n_{\downarrow}(E) \sim (V_{\mathrm{SO}}^{\downarrow\uparrow})^2$. At the band edges this simplified picture is modified by the fact that here, unperturbed spin-up and-spin down bands cross and higher order perturbation theory has to be taken into account. As a measure of the strength of the half metallicity it is possible to consider the spin polarization at the Fermi level

$$P = \frac{n_{\uparrow}(E_F) - n_{\downarrow}(E_F)}{n_{\uparrow}(E_F) + n_{\downarrow}(E_F)}, \tag{4}$$

which reflects the strength of the spin orbit induced spin-flip scattering at the Fermi energy. In the ideal case with $n_{\downarrow}(E_F)=0$ this quantity should be 100%. For the considered Heusler structures the spin polarization is close to 100% for Co_2MnSi and 96.5% for Co_2MnGe. The lower spin polarization for Co_2MnGe is consistent with the slightly larger spin orbit coupling constant determined within the ETH-TB model. Therefore the contributions from the down spin channel in Eq. (3) will contribute more significantly for Co_2MnGe than for Co_2MnSi and which is shown in Figs. 3(a) and 3(b), where in addition to the total damping the contributions generated from $S_{mn}^{\uparrow\uparrow}(\boldsymbol{k})+S_{mn}^{\downarrow\uparrow}(\boldsymbol{k})$ as well as from $S_{mn}^{\uparrow\uparrow}(\boldsymbol{k})$ are calculated. As expected the contributions from $S_{mn}^{\downarrow\downarrow}(\boldsymbol{k})$ are negligible for Co_2MnSi. We note that the lowest experimental value of Gilbert damping, which we are aware of, was measured for the half-metallic half Heusler NiMnSb,[22] which is consistent with the high spin polarization calculated for this material in Ref. 21.

In summary we have developed a model combining first-principles calculations and an ETH-TB model that enables the calculation of the magnetization relaxation in a wide variety of materials. The model also allows to analytically trace the origin of the Gilbert damping in these materials. The predicted dependence for the damping parameter on the electric resistivity of the material will facilitate a direct comparison with future experimental results. The insight provided by this approach will allow further development of low damping materials for future spintronic applications.

We would like to thank K. Gilmore for the stimulating discussion and R. Lopez for his detailed help regarding the development of the described ETH-TB code. This work was partly supported by NSF (Grant Nos. DMR 0213985, DMR 0213985, ECCS-529369, and DMR 0804243) and by the Information Storage Industry Consortium.

[1] L. Landau and E. Lifshitz, Phys. Z. Sowjetunion **8**, 153 (1935).
[2] T. L. Gilbert, Phys. Rev. **100**, 1243 (1955).
[3] T. L. Gilbert, IEEE Trans. Magn. **40**, 3443 (2004).
[4] K. Gilmore, Y. U. Idzerda, and M. D. Stiles, Phys. Rev. Lett. **99**, 027204 (2007).
[5] K. Gilmore, Y. U. Idzerda, and M. D. Stiles, J. Appl. Phys. **103**, 07D303 (2008).
[6] V. Kamberský, Phys. Rev. B **76**, 134416 (2007).
[7] B. Heinrich, D. Fraitová, and V. Kamberský, Phys. Status Solidi **23**, 501 (1967).
[8] V. Kamberský, Can. J. Phys. **48**, 2906 (1970).
[9] V. Kamberský, Czech. J. Phys., Sect. B **26**, 1366 (1976).
[10] J. Cerdá and F. Soria, Phys. Rev. B **61**, 7965 (2000).
[11] C. M. Goringe, D. R. Bowler, and E. Hernández, Rep. Prog. Phys. **60**, 1447 (1997).
[12] R. Hoffmann, Rev. Mod. Phys. **60**, 601 (1988).
[13] J. F. Cochran and B. Heinrich, IEEE Trans. Magn. **16**, 660 (1980).
[14] B. Heinrich, D. J. Meredith, and J. F. Cochran, J. Appl. Phys. **50**, 7726 (1979).
[15] G. Kresse and J. Hafner, Phys. Rev. B **47**, 558 (1993).
[16] R. S. Mulliken, C. A. Rieke, D. Orloff, and H. Orloff, J. Chem. Phys. **17**, 1248 (1949).
[17] M. Wolfsberg and L. Helmholz, J. Chem. Phys. **20**, 837 (1952).
[18] L. Ritchie, G. Xiao, Y. Ji, T. Y. Chen, C. L. Chien, M. Zhang, J. Chen, Z. Liu, G. Wu, and X. X. Zhang, Phys. Rev. B **68**, 104430 (2003).
[19] J.-M. André, J. Delhalle, G. Kapsomenos, and G. Leroy, Chem. Phys. Lett. **14**, 485 (1972).
[20] Ph. Mavropoulos, K. Sato, R. Zeller, P. H. Dederichs, V. Popescu, and H. Ebert, Phys. Rev. B **69**, 054424 (2004).
[21] Ph. Mavropoulos, I. Galanakis, V. Popescu, and P. H. Dederichs, J. Phys.: Condens. Matter **16**, S5759 (2004).
[22] B. Heinrich, G. Woltersdorf, R. Urban, O. Mosendz, G. Schmidt, P. Bach, L. Molenkamp, and E. Rozenberg, J. Appl. Phys. **95**, 7462 (2004).